Journal of Paleontology, 96(5), 2022, p. 1149–1165

Published by Cambridge University Press
on behalf of The Paleontological Society
0022-3360/22/1937-2337
doi: 10.1017/jpa.2022.26

JOURNAL OF PALEONTOLOGY
A PUBLICATION OF THE Paleontological SOCIETY

Revision of *Histiodella labiosa* Bauer, 2010, and its inferred phylogeny in the evolution of the Middle Ordovician conodont genus *Histiodella* Harris, 1962

Yong Yi Zhen,[1]* Jeffrey A. Bauer,[2] and Stig M. Bergström[3]

[1]Geological Survey of New South Wales, W.B. Clarke Geoscience Centre, 947-953 Londonderry Rd/Londonderry, NSW 2753, Australia <yong-yi.zhen@planning.nsw.gov.au>
[2]Shawnee State University, 940 Second Street Portsmouth, OH 45662, USA <jbauer@shawnee.edu>
[3]School of Earth Sciences, The Ohio State University, 125 S. Oval Mall, Columbus, Oh 43210, USA <Bergstrom.1@osu.edu>

Abstract.—Based on abundant topotype specimens from the Oil Creek Formation at the type locality in southern Oklahoma, *Histiodella labiosa* is described and revised. The morphological variation of the Pa, Pb, and M elements of this previously little-known species is also systematically documented and illustrated. The revised species definition, with formal designation of a lectotype and a new diagnosis supported by morphological comparison with its ancestral and descendent species, has enhanced its value for correlation of the lower Darriwilian. The inferred phylogeny of *Histiodella* that resulted from this study is based on both cladistic and morphological analyses. It supports the monophyletic grouping of *Histiodella* species and their evolutionary relationships. This has wide biostratigraphic implications because many *Histiodella* species are valuable for detailed global correlation of upper Dapingian to middle Darriwilian strata.

Introduction

The conodont species *Histiodella labiosa* Bauer, 2010, was erected based on a large collection of ~997 specimens from 27 samples from the middle to upper part of the Oil Creek Formation exposed near US Highway 77 and Interstate 35 in southern Oklahoma (Fig. 1). Based on the distinctive morphological features of this species, Bauer (2010) established the *H. labiosa* Biozone in the Oil Creek Formation for a stratigraphic interval between the *H. sinuosa* and *H. holodentata* biozones. However, outside North America, *H. labiosa* has only been recorded from the lower Darriwilian in Australia. It is likely that the morphological entity represented by *H. labiosa* was lumped either in *H. holodentata* Ethington and Clark, 1982, or in *H. serrata* Harris, 1962. To overcome this drawback and inconsistencies in taxonomy, *H. labiosa* is revised herein based on the study of originally illustrated types of this species, including a newly selected lectotype (Bauer, 2010, pl. 2, fig. 13), other paralectotypes (Bauer, 2010, pl. 2, figs. 10, 11, 14), and re-examination of the original and additional topotype material from the type locality. Abundant topotype material of *H. labiosa* has illustrated the morphological variation of its Pa, Pb, and M elements. Detailed study of this morphological variation allows us to analyze the phylogenetic relationships of *H. labiosa* with its closely related species and to better elucidate the evolution of the *Histiodella* species through late Dapingian to middle Darriwilian during the Middle Ordovician.

*Corresponding author.

Geological setting and regional stratigraphy

The Arbuckle Mountains region of southern Oklahoma contains one of the best and most-continuous exposures (nearly 3350 m in total thickness) of fossiliferous upper Cambrian to Devonian rocks in the Midcontinent of the United States (Ham, 1973; Carlucci et al., 2015). The sequences were uplifted regionally in association with folding and faulting during the Ouachita Orogeny, a mountain building event in the Pennsylvanian and Permian (Thomas, 1991; Ettensohn et al., 2019).

The Simpson Group is a Middle to Late Ordovician carbonate and clastic succession reaching a maximum thickness of >760 m. It is widely distributed in southern Oklahoma and extends farther southwest into West Texas and southeastern New Mexico. In southern Oklahoma, the Simpson Group includes, in ascending order, the Joins, Oil Creek, McLish, Tulip Creek, and Bromide formations (Decker and Merritt, 1931). It was deposited during a major marine transgression and followed deposition of the upper (Lower to lowest Middle Ordovician) Arbuckle Group (Derby et al., 1991; Ethington et al., 2012; Morgan, 2012; Read and Repetski, 2012; Taylor et al., 2012). The Middle and Upper Ordovician are characterized by intervals of predominantly shales and clay-rich carbonates deposited during maximum flooding, whereas sandstone dominates intervals laid down during the low standing of sea level fluctuations.

The Joins Formation, with a total thickness of close to 90 m, is primarily thin- to medium-bedded limestone with shale interlayers that overlies (locally unconformable) the West Spring Creek Formation of the Arbuckle Group of latest Cambrian to earliest Middle Ordovician age (Derby et al., 1991; Ethington et al., 2012; Morgan, 2012; Taylor et al., 2012). The

Figure 1. Location maps showing the study area in Oklahoma of the USA (**1**), location of study area in southern Oklahoma (**2**), and (**3**) the detailed location of the sampled section (marked by *) of the Oil Creek Formation with samples from the section bearing designations 72SC (collected by Bergström, Jaanusson, and Sweet in 1972) and 89JA (collected by Bauer in 1989), which is exposed near US Highway 77 and Interstate 35 in southern Oklahoma.

conformably succeeding Oil Creek Formation, with a maximum thickness of just over 300 m, consists of a lower sandstone member and an upper limestone member of thin- to medium-bedded limestone and interbedded greenish gray shales that gradationally become more dominant towards the top (Henry, 1988). At the type locality (section 72SC) of *H. labiosa*, which is the focus of this study, the Oil Creek Formation has a total thickness of 193 m (Fig. 2).

As the type localities and type strata of several species of *Histiodella* Harris, 1962, the Joins Formation and the overlying Oil Creek Formation in the Arbuckle Mountains region are fundamentally important in the study of this morphologically distinctive Middle Ordovician conodont genus. These two carbonate-dominated units of southern Oklahoma may represent the most continuous Middle Ordovician succession in the world that yields abundant material of several *Histiodella* species. They have been the focus of several classical works in the past six decades (e.g., Harris, 1962; Mound, 1965; McHargue, 1975, 1982; Bauer, 2010), particularly to study species of *Histiodella* in establishing a finely defined biozonal scheme,

https://doi.org/10.1017/jpa.2022.26 Published online by Cambridge University Press

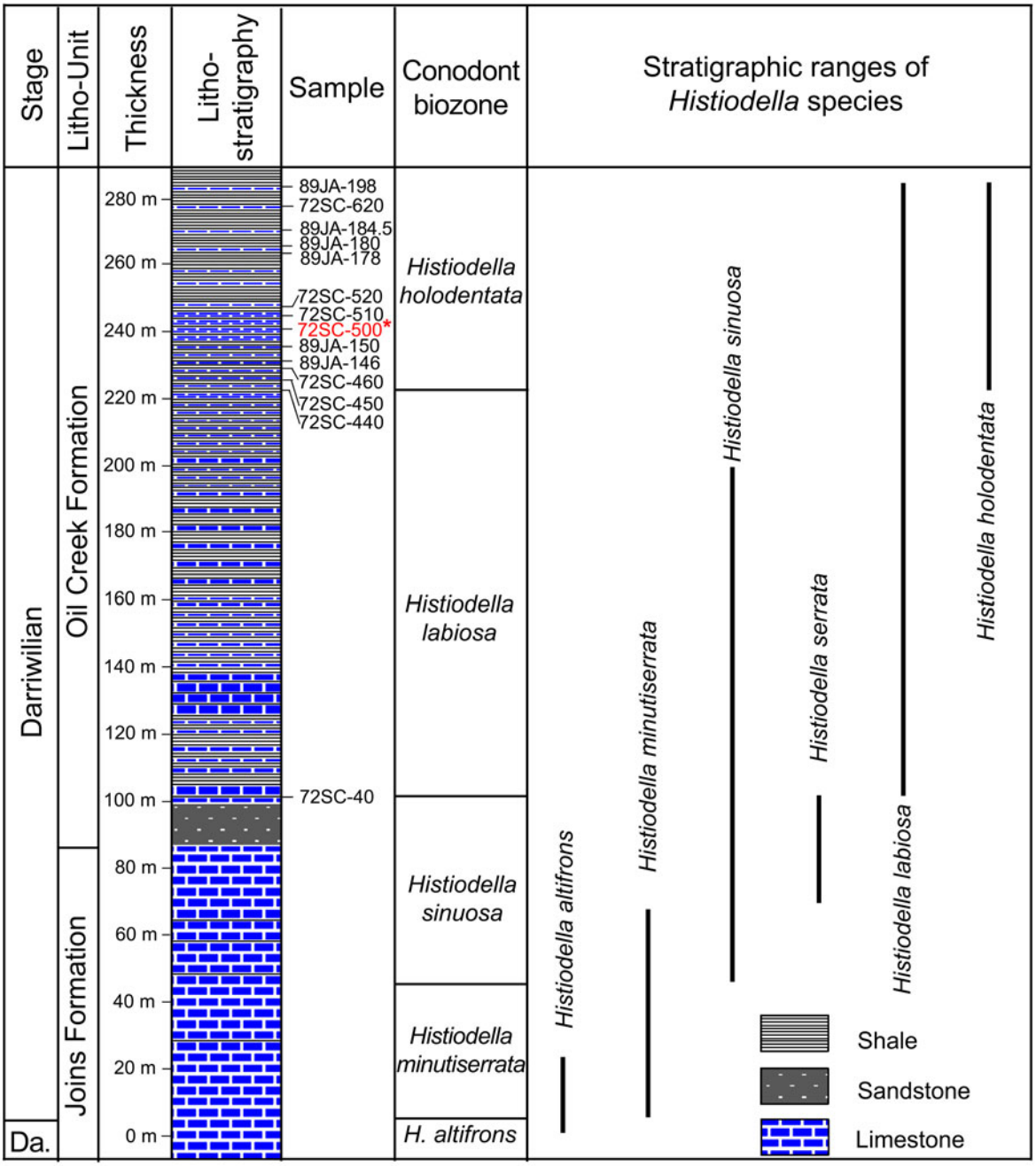

Figure 2. Composite stratigraphic section of the 72SB (Joins Formation) and 72SC (Oil Creek Formation) showing the stratigraphic horizon of the lectotype (from sample 72SC-500, marked with red font and a red star) and horizons of the 10 conodont samples examined in this study. Conodont biozones and stratigraphic occurrences and ranges of *Histiodella* species recognized in the Joins and Oil Creek formations at this section in southern Oklahoma are based on Bauer (2010). Da. = Dapingian.

which is now widely used to subdivide the late Dapingian to middle Darriwilian strata worldwide (Bergström and Ferretti, 2017; Goldman et al., 2020; Zhen, 2021).

Materials and methods

The topotypes of *H. labiosa* used in this study represent a total of 427 discrete specimens recovered from four samples from the Oil Creek Formation. They include sample 72SC-450 (137.16 m above the base of the Oil Creek Fm., with 128 specimens recovered), sample 72SC-460 (140.21 m above the base of the Oil Creek Fm., with 53 specimens recovered), sample 72SC-510 (155.45 m above the base of the Oil Creek Fm., with 79 specimens recovered), and sample 72SC-520 (158.5 m above the base of the Oil Creek Fm., with 167 specimens recovered). Section 72SC starts at coordinates 34.365000°N, 97.145833°W, and ends at the top of the Oil Creek Formation at coordinates 34.362500°N, 97.146667°W. The section is exposed in several low ridges between US Highway 77 and Interstate 35 (SE1/4, sec. 24, T.2S., R.1E., Carter County), in

https://doi.org/10.1017/jpa.2022.26 Published online by Cambridge University Press

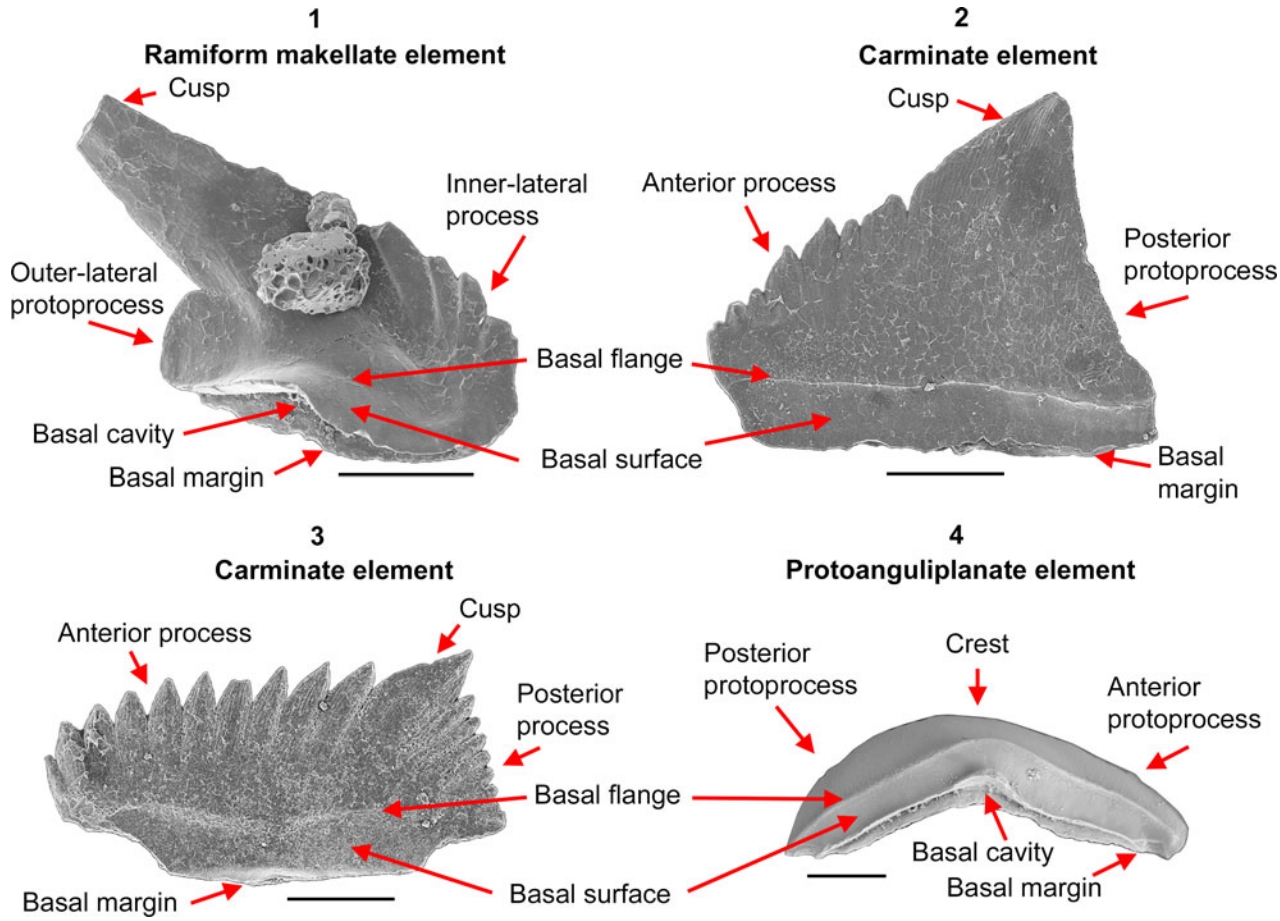

Figure 3. Orientation, morphology, and structural terms for *Histiodella* and related genera: (**1**) M element of *Histiodella labiosa* Bauer, 2010; (**2**) Pb element of *Histiodella labiosa* Bauer, 2010; (**3**) Pa element of *Histiodella holodentata* Ethington and Clark, 1982; (**4**) Protoanguliplanate P element of *Cooperignathus nyinti* (Cooper, 1981). All scale bars represent 100 µm.

southern Oklahoma. The lectotype (Bauer, 2010, pl. 2, fig. 13) is from sample 72SC-500, collected 152.4 m above the base of the Oil Creek Fm., with 75 specimens of *H. labiosa* recovered. They represent the most productive samples of *H. labiosa* among the 27 samples that yielded this species when Bauer (2010) originally studied and erected *H. labiosa*. All samples were collected by S.M. Bergström, the late V. Jaanusson, and the late Prof. W.C. Sweet in 1972. Topotype material of *H. labiosa* was recovered by Jeffrey A. Bauer in 1989 in a nearby section exposed along the east side of Interstate 35 (Fig. 2) from six additional samples: 89JA-178 (175 m above the base of the Oil Creek Fm., with 310 specimens recovered), 89JA-184.5 (181.5 m above the base of the Oil Creek Fm., with six specimens recovered), 89JA-180 (177 m above the base of the Oil Creek Fm., with seven specimens recovered), 89JA-150 (147 m above the base of the Oil Creek Fm., with two specimens recovered), 89JA-146 (143 m above the base of the Oil Creek Fm., with one specimen recovered), and 89JA-198 (195 m above the base of the Oil Creek Fm., with one specimen recovered). The S and M elements of the *Histiodella* species are generally smaller than the Pa and Pb elements. Repetski (personal communication, 2021) indicated that a 200-mesh bottom sieve would catch S and M elements, whereas most or all of these elements would pass through a 140-mesh sieve. When the samples of this study were processed, unfortunately a 140-mesh sieve was used, which might be responsible for the bias of the element types recovered.

Repository and institutional abbreviation.—Thirty topotype specimens of *H. labiosa* illustrated in Figures 3–6 bearing the prefix OSU (OSU 54951–54980, inclusive) are deposited in the Type Collection of the Orton Geological Museum, Orton Hall, School of Earth Sciences, The Ohio State University, Columbus, USA. All images illustrated are SEM digital photomicrographs (numbers with the prefix IY are the file names of the digital images).

Systematic paleontology

Morphological and apparatus notational terms defined in the conodont Treatise (Clark et al., 1981) are followed in this contribution, except for the following technical terms, which are briefly defined herein (Fig. 3).

Basal flange.—A costa-like structure presented as a prominent shelf-like projection, which extends around the element parallel

https://doi.org/10.1017/jpa.2022.26 Published online by Cambridge University Press

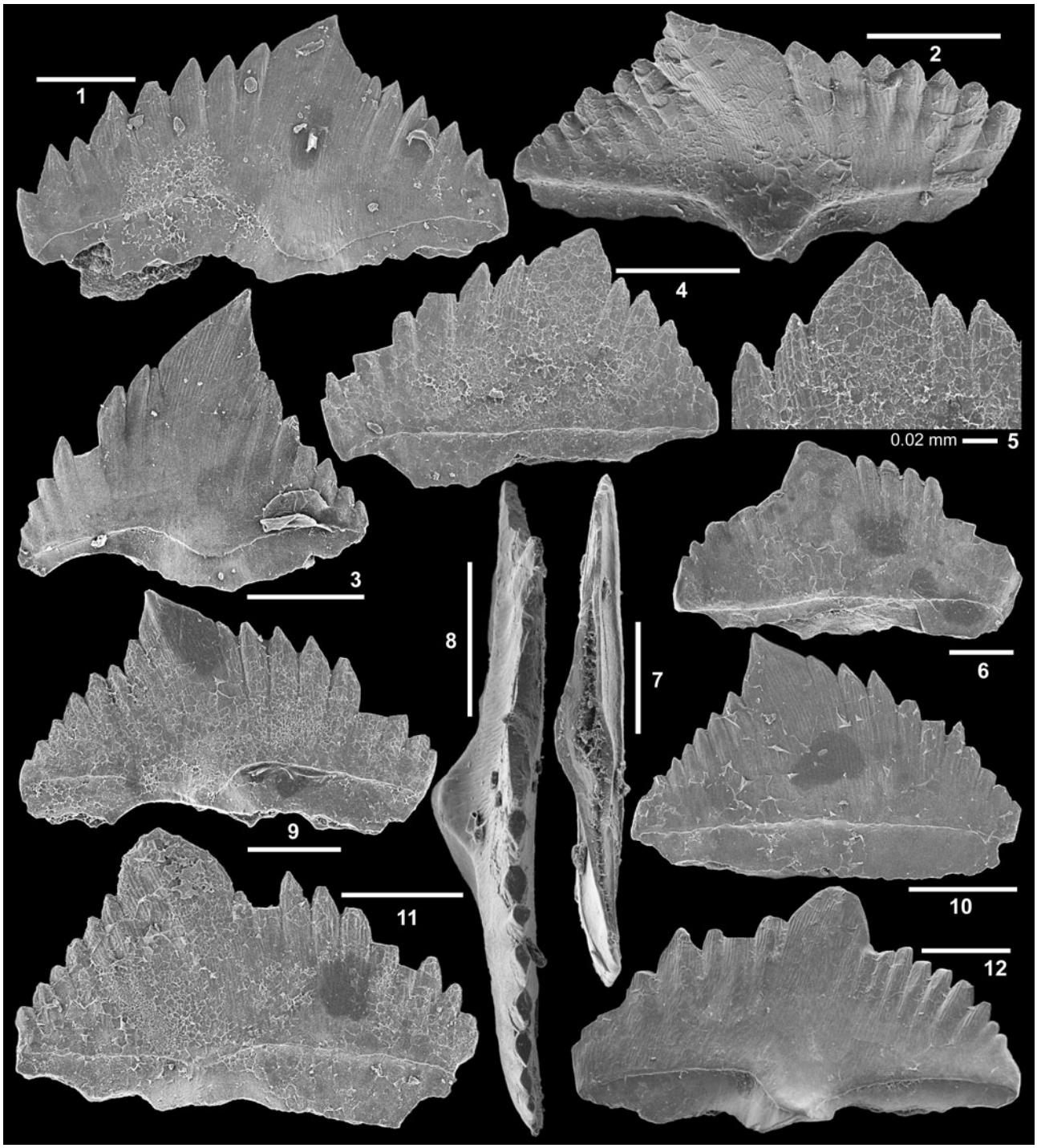

Figure 4. *Histiodella labiosa* Bauer, 2010, from the Oil Creek Formation in the section 72SC exposed in southern Oklahoma: Pa element. (**1**) OSU 54951, 72SC-450, inner-lateral view (IY406-15); (**2**) OSU 54952, 72SC-520, apical-outer-lateral view (IY406-03); (**3**) OSU 54953, 72SC-460, outer-lateral view (IY406-17); (**4, 5**) OSU 54954, 72SC-510, (**4**) inner-lateral view (IY406-29), (**5**) close up showing surface striation (IY406-30); (**6**) OSU 54955, 72SC-520, inner-lateral view (IY406-01); (**7**) OSU 54956, 89JA-178, basal view (IY416-19); (**8**) OSU 54957, 89JA-178, apical view (IY416-05); (**9**) OSU 54958, 72SC-510, outer-lateral view (IY406-22); (**10**) OSU 54959, 72SC-510, inner-lateral view (IY406-23); (**11**) OSU 54960, 72SC-520, outer-lateral view (IY406-02); (**12**) OSU 54961, 89JA-178, outer-lateral view (IY416-01). All scale bars represent 100 µm, unless otherwise indicated.

to, and slightly above, the basal margin to define the upper limits of the basal surface. This character is well developed in species of *Cooperignathus*, *Jumudontus*, and *Histiodella*, as well as in some species of *Protoprioniodus*, *Oelandodus* (likely a junior synonym of *Protoprioniodus*), and *Fahraeusodus*.

Basal surface.—The surface adjacent to the basal margin of the elements located between the basal margin and the basal flange.

Makellate element.—A term referring to most types of the elements taking the M position in the apparatus. The

https://doi.org/10.1017/jpa.2022.26 Published online by Cambridge University Press

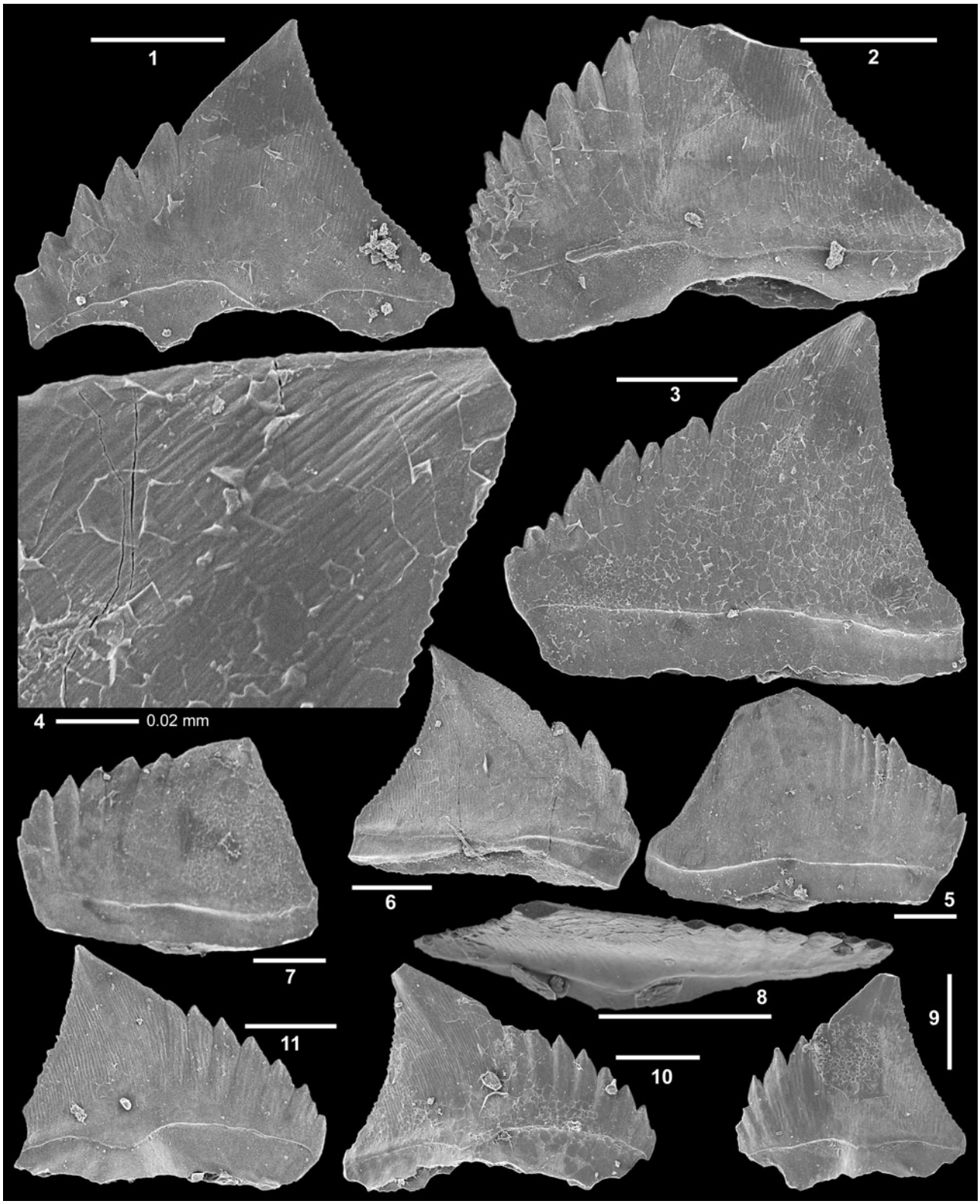

Figure 5. *Histiodella labiosa* Bauer, 2010, from the Oil Creek Formation in the section 72SC exposed in southern Oklahoma: Pb element. (**1**) OSU 54962, 72SC-460, outer-lateral view (IY406-06); (**2**) OSU 54963, 72SC-520, inner-lateral view (IY406-06); (**3, 4**) OSU 54964, 72SC-510, (**3**) inner-lateral view (IY406-25), (**4**) close up showing minutely serrated posterior edge (IY406-26); (**5**) OSU 54965, 72SC-450, inner-lateral view (IY406-14); (**6**) OSU 54966, 72SC-460, outer-lateral view (IY406-21); (**7**) OSU 54967, 72SC-520, inner-lateral view (IY406-09); (**8**) OSU 54968, 89JA-178, apical view (IY416-13); (**9**) OSU 54969, 89JA-178, outer-lateral view (IY416-17); (**10**) OSU 54970, 89JA-178, outer-lateral view (IY416-12); (**11**) OSU 54971, 72SC-460, outer-lateral view (IY406-20). All scale bars represent 100 µm, unless otherwise indicated.

https://doi.org/10.1017/jpa.2022.26 Published online by Cambridge University Press

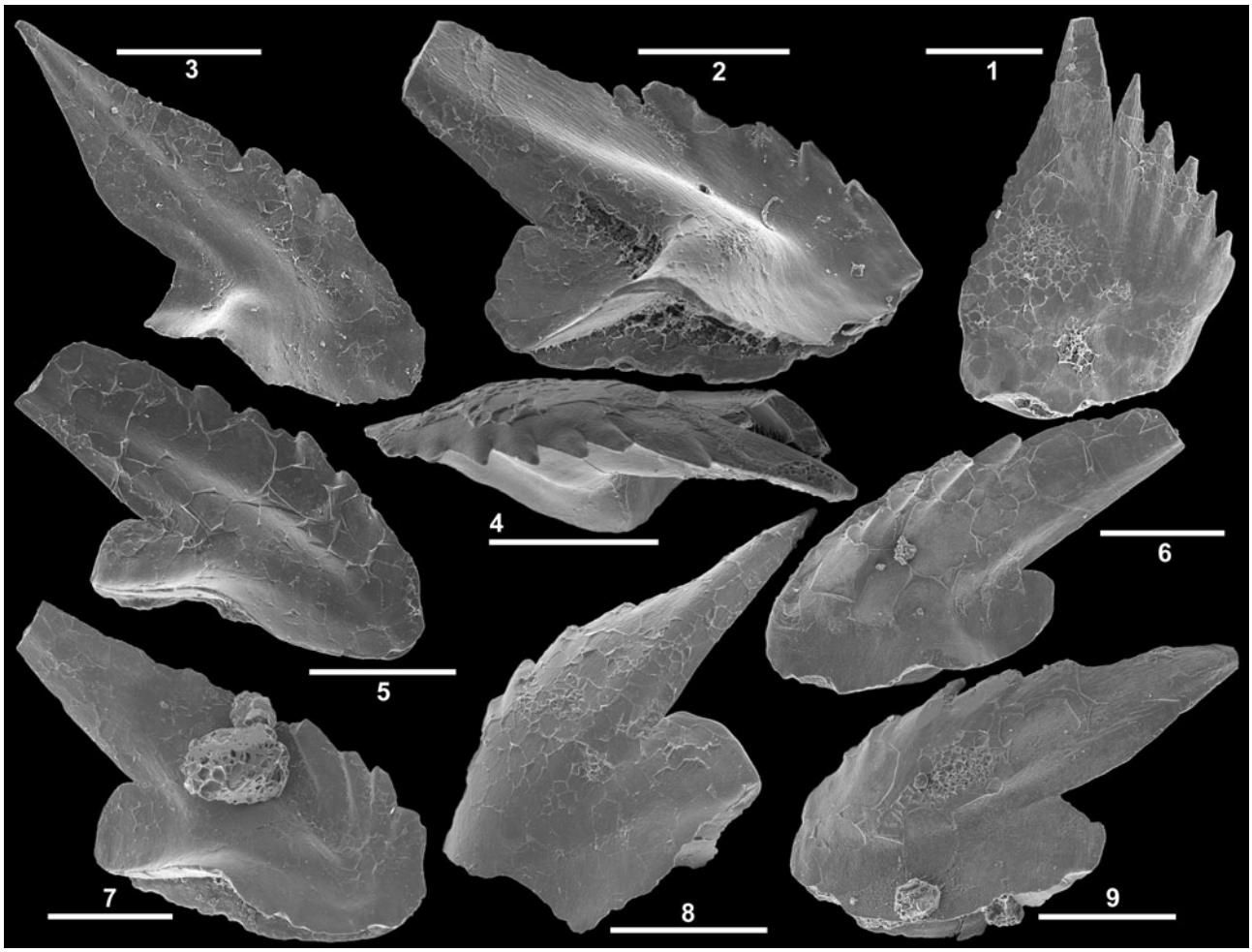

Figure 6. *Histiodella labiosa* Bauer, 2010, from the Oil Creek Formation in the section 72SC exposed in southern Oklahoma. (**1**) Sc element, OSU 54972, 89JA-178, outer-lateral view (IY416-20); (**2–9**) M element: (**2**) OSU 54973, 89JA-178, basal-posterior view (IY416-24); (**3**) OSU 54974, 72SC-510, posterior view (IY406-28); (**4**) OSU 54975, 89JA-178, apical view (IY416-27); (**5**) OSU 54976, 89JA-178, posterior view (IY416-30); (**6**) OSU 54977, 89JA-178, posterior view (IY416-29); (**7**) OSU 54978, 89JA-178, posterior view (IY416-25); (**8**) OSU 54979, 89JA-178, anterior view (IY416-26); (**9**) OSU 54980, 89JA-178, anterior view (IY416-28). All scale bars represent 100 µm.

most distinctive feature of a makellate element is its orientation as an antero-posteriorly compressed ramiform, protoramiform, or coniform element (Sweet, 1988; Nicoll, 1990, 1992).

Protoprocess.—Adentate anterior, posterior, or lateral projections of protoramiform, ramiform, protopectiniform, or pectiniform elements.

Protocarminate element.—A blade-like protopectiniform element with a prominent cusp, posterior and anterior protoprocesses, and a straight or nearly straight basal margin.

Protoanguliplanate element.—An arched protopectiniform element with the upper surface developed as a thin, antero-posteriorly extended, blade-like crest, which lacks a recognizable cusp and denticles; typically represented by the P element of *Cooperignathus nyinti* (Cooper, 1981) and *C. aranda* (Cooper, 1981).

Class Conodonta Pander, 1856
Order Ozarkodinida Dzik, 1976
Suborder Plectodinida Dzik, 1991
Superfamily Oistodontacea Lindström, 1970
Family Oistodontidae Lindström, 1970
Genus *Histiodella* Harris, 1962

Type species.—*Histiodella altifrons* Harris, 1962.

Diagnosis.—Seximembrate (or septimembrate) apparatus of adentate (in early species) to denticulate (in later species) elements, including geniculate makellate M element, protoramiform or ramiform S elements, which form a symmetry transition series from alate prototriform or triform Sa, asymmetrical prototertiopedate (or modified tertiopedate) Sb, to asymmetrical and laterally compressed protobipennate or modified bipennate Sc and possibly protoquadriramate or quadriramate Sd, and protocarminate or carminate P elements typically with well-defined basal surface between the basal flange and basal margin (modified after McHargue, 1982, p. 1430–1431, and Stouge, 2012, p. 82).

https://doi.org/10.1017/jpa.2022.26 Published online by Cambridge University Press

Remarks.—Two species of *Histiodella,* including the type species of the genus (*H. altifrons*) and *H. serrata*, were erected by Harris (1962) as form species based on the Pa elements (protocarminate for *H. altifrons* and carminate for *H. serrata*) from the Joins Formation exposed in the Arbuckle Mountains of southern Oklahoma. Harris (1962, p. 209) distinguished the latter by its larger size with denticulate upper margin of the anterior and posterior processes. Mound (1965) subsequently erected *H. minutiserrata* and *H. triquetra* as two additional form species from the Joins Formation of the Arbuckle Mountains, Oklahoma. The former was based on the protocarminate Pa element differing from *H. altifrons* in having a minutely serrated upper margin, and *H. triquetra* was based on the prototriform alate element. *Histiodella sinuosa* (Graves and Ellison, 1941) was established as a form species based on the carminate Pa element characterized by having a denticulate anterior process and adentate posterior process. The type material of *H. sinuosa*, which is from the Fort Peña Formation of West Texas (Graves and Ellison, 1941; Bradshaw, 1969), was also reported from upper part of the Joins Formation and lower and middle part of the Oil Creek Formation in Arbuckle Mountains of southern Oklahoma (McHargue,1982; Bauer, 2010) and correlative units in Utah (Ethington and Clark, 1982) and Nevada (Harris et al., 1979; Sweet et al., 2005) of North America. Bradshaw (1969) adopted a broader species concept of *H. sinuosa* and synonymized all the known species of *Histiodella* at the time, including *H. altifrons* Harris, 1962, *H. serrata* Harris, 1962, *H. minutiserrata* Mound, 1965, and *H. triquetra* Mound, 1965.

McHargue (1975, 1982) was the first to apply a multielement species concept to the species of *Histiodella* based on the study of a large collection from the Joins Formation in the Arbuckle Mountains, southern Oklahoma. Although Pb (= short bryantodontiform of McHargue, 1982), ramiform S (including Sa, Sb, and Sc = trichonodelliform, zygognathiform, and twisted bryantodontiform, respectively, of McHargue, 1982) and geniculate makellate M (= oistodontiform of McHargue, 1982) elements were recognized to form the species apparatuses (McHargue, 1982, text-fig. 2), the seximembrate species concept and distinction among the four species (*H. altifrons*, *H. minutiserrata*, *H. serrata*, and *H. sinuosa*) recovered from the Joins Formation were mainly based on the protocarminate or carminate Pa elements (= bryantodontiform of McHargue, 1982) of these species, because the S elements were much less frequently represented in the Joins Formation samples and were difficult to assign confidently to species based on their morphology and known stratigraphic range (McHargue, 1982, table 1).

Ethington and Clark (1982) accepted the species concept proposed by McHargue (1982) and recovered *H. altifrons*, *H. minutiserrata*, and *H. sinuosa* from the Kanosh Shale, and a new species, *H. holodentata* Ethington and Clark, 1982, from the overlying Lehman Formation of Utah. Similarly, the 516 original type specimens defining *H. holodentata* from the Ibex area belong to the carminate Pa element, except for a single ramiform element assignable to the triform Sa element. Subsequently, three species of *Histiodella*, including *H. bellburnensis* Stouge, 1984, *H. kristinae* Stouge, 1984, and *H. tableheadensis* Stouge, 1984 (a junior synonym of *H. holodentata*) were erected based on the material from the Table Head Group of Newfoundland. Stouge (1984, p. 87) suggested that the apparatuses of the *Histiodella* species from the Table Head Group consisted of six morphologically distinctive elements, but the Pb (= ozarkodiniform element of Stouge, 1984), geniculate M, and ramiform S elements were relatively rare, smaller in size, and were neither adequately described nor illustrated. Among these three species recognized in the Table Head Group, *H. bellburnensis* is represented by only the carminate Pa element (Stouge, 1984, p. 87, pl. 17, figs. 20, 21), *H. tableheadensis* by the carminate Pa (Stouge, 1984, p. 87, 88, pl. 18, figs. 8, 12–14) and unillustrated geniculate M and ramiform S elements, and *H. kristinae* by the carminate Pa (Stouge, 1984, p. 87, pl. 18, figs. 2, 3, 6, 7), geniculate M (Stouge, 1984, p. 87, pl. 18, figs. 1, 4), and ramiform S (Stouge, 1984, p. 87, pl. 18, figs. 5, 9–11) elements.

Several species of *Histiodella* were also erected from the middle Darriwilian of North China, but they were based solely on the carminate Pa elements. *Histiodella triangularis* (Wang and Lou, 1984) and *H. wuhaiensis* Wang, Bergström, Zhen, Zhang, Wu, and Chen, 2013, were characterized by having an inconspicuous cusp and are considered as valid, showing closer phylogenetic ties with *H. bellburnensis*. *Histiodella infrequensa* An in An et al., 1983, from the Beianzhuang Formation of North China is considered as a junior synonym of *H. holodentata*, and *H. intertexa* An in An et al., 1981 (illustrated only as a nomen nudum in An et al., 1981, 1985, and formally defined in An, 1987) from the Kuniutian Formation in South China as a junior synonym of *H. kristinae*. A likely new species recently reported from middle Darriwilian cherts in New South Wales and referred to as *Histiodella* sp. cf. *H. kristinae* is also solely based on the carminate Pa element, which is like that of *H. kristinae*, but with a more extended anterior process (Zhen and Rutledge, 2020, fig. 10g–i; Zhen et al., 2021b, fig. 5s).

It is now generally agreed that *Histiodella* species have a seximembrate or septimembrate apparatus, a view supported by recovery of Pb, M, and S elements in association with various species of *Histiodella*, as discussed above (e.g., Ethington and Clark, 1982; McHargue, 1982; Stouge, 1984, 2012; Sweet, 1988; Zhen and Percival, 2004; Du et al., 2005; Bauer, 2010; Feltes et al., 2016). However, their morphologic relationships within an apparatus, particularly between the rare and delicate ramiform S elements and the constituent Pa element, are still poorly understood and often variably interpreted. Therefore, differentiation of a *Histiodella* species is practically still based mainly, if not solely, on the Pa element.

Histiodella donnae Repetski, 1982, from the lower part (upper Tremadocian) of the El Paso Group of westernmost Texas, is represented by a symmetrical element (figured paratype, Repetski, 1982, pl. 8, fig. 7; interpreted herein as representing the Sa element) and an asymmetrical element (holotype, Repetski, 1982, pl. 8, fig. 6; interpreted herein as representing the Sb element). Two additional elements belonging to this species subsequently were illustrated by Repetski et al. (1998, fig. 2I–L), including a geniculate M (Repetski et al., 1998, fig. 2J) and a laterally compressed coniform Sc (Repetski et al., 1998, fig. 2L). A posteriorly curved cusp and a mid-carina on the broadly concave posterior face of the Sa and Sb elements of *H. donnae* suggest a closer phylogenetic relationship with *Rossodus* Repetski and Ethington, 1983. However, because the P

https://doi.org/10.1017/jpa.2022.26 Published online by Cambridge University Press

elements have not been recovered for *H. donnae*, the morphological and phylogenetic relationship between these leaf-shaped blades of *H. donnae* and *Histiodella* sensu stricto from the Middle Ordovician remains unclear. Therefore, *H. donnae* is excluded herein from *Histiodella* sensu stricto. *Histiodella angulata* Moskalenko, 1982 (see Moskalenko, 1983; Tolmacheva et al., 2019), reported from lower Darriwilian of the Siberian Platform, is considered herein as a possible species of *Jumudontus* Cooper, 1981. *Histiodella levis* Tolmacheva, 2014, from the lower Darriwilian of central Asia is an adentate species consisting of a seximembrate apparatus that is comparable with that of *H. altifrons*, but the Pa element of *H. levis* (see Tolmacheva, 2014, pl. 22, figs. 1–9, 18) has a much shorter anterior protoprocess, a more open basal cavity, a prominent platform-like projection on the outer-lateral side, and surface granular ornamentation on the basal flange and basal surface, which resemble typical *Jumudontus* species. More specifically, the strong resemblance between the granular ornamentation (Tolmacheva, 2014, pl. 22, fig. 18) of *H. levis* and the small pustules developed on the P elements of *Jumudontus gananda*, as documented by Nicoll (1992), suggests a closer relationship of these species.

Species assigned to Histiodella.—Given the remarks above, only the 10 named species discussed below are confirmatively included in *Histiodella*.

Histiodella altifrons Harris, 1962.—Middle Ordovician, holotype (OMC 115, figured by Harris, 1962, pl. 1, fig. 4) from the horizon 11.89 m (39 feet) above the base of the Joins Formation at the Simpson section located along the west side of U.S. Highway 77, on the south side of Arbuckle Mountains, Oklahoma (= *Histiodella triquetra* Mound, 1965).

Histiodella bellburnensis Stouge, 1984.—Middle Darriwilian, holotype (ROM 39716, figured by Stouge, pl. 17, fig. 20) from the Middle Member of the Table Head Group exposed at Table Point of the Great Northern Peninsula, Newfoundland.

Histiodella holodentata Ethington and Clark, 1982.—Middle Darriwilian, holotype (UMC 1094-2, figured by Ethington and Clark, 1982, pl. 4, fig. 3) from the Lehman Formation in the Ibex area of western Utah (= *Histiodella infrequensa* An in An et al., 1983; = *Histiodella tableheadensis* Stouge, 1984). A morphologically transitional form between *H. holodentata* and *H. kristinae* is characterized by having the tips of the cusp and the tallest denticle on the anterior process at more or less the same height. This form was treated by Stouge (2012) as a separate species, referred to as *Histiodella* cf. *holodentata*, while other authors (e.g., Zhen, 2020; Zhen et al., 2020a) considered it as representing an advanced variant of *H. holodentata.*

Histiodella kristinae Stouge, 1984.—Middle Darriwilian, holotype (ROM 39718, figured by Stouge, pl. 18, fig. 3) from the Middle Member of the Table Head Group exposed at Table Point of the Great Northern Peninsula, Newfoundland (= *H. intertexa* An in An et al., 1981, which was introduced as a nomen nudum).

Histiodella labiosa Bauer, 2010.—Early Darriwilian, lectotype (hereby specimen OSU 52034, originally figured by Bauer, 2010, pl. 2, fig. 13, is designated as lectotype) from sample 72SC-500 at the horizon 152.4 m above the base of the Oil Creek Formation in section 72SC exposed in southern Oklahoma.

Histiodella minutiserrata Mound, 1965.—Middle Ordovician, holotype (USNM 146971, figured by Mound, 1965, pl. 3, fig. 2) from the Joins Formation at the Simpson section (same locality and section of Harris, 1962, as indicated by Mound, 1965, p. 2) located along the west side of U.S. Highway 77, on the south side of the Arbuckle Mountains, Oklahoma.

Histiodella serrata Harris, 1962.—Middle Ordovician, holotype (OMC 118, figured by Harris, 1962, pl. 1, fig. 3) from the horizon 57 m (187 feet) above the base of the Joins Formation at the Simpson section, located along the west side of U.S. Highway 77, on the south side of the Arbuckle Mountains, Oklahoma (= ?*Histiodella triquetra* Mound, 1965, which might represent the Sa element of *H. serrata*).

Histiodella sinuosa (Graves and Ellison, 1941).—Middle Ordovician, holotype (MSM 7125, G414, figured by Graves and Ellison, 1941, pl. 2, fig. 13) from the Fort Peña Formation exposed on east side of road in bed of Alsate Creek, six miles southwest of Marathon, Texas.

Histiodella triangularis (Wang and Lou, 1984).—Middle Darriwilian, holotype (NIGP 52199, figured by Wang and Lou, 1984, pl. 12, fig. 17) from the Zotzeshan Formation of Inner Mongolia, North China.

Histiodella wuhaiensis Wang, Bergström, Zhen, Zhang, Wu, and Chen, 2013.—Middle Darriwilian, holotype (NIGP 156446, figured by Wang et al., 2013, pl. 2, fig. 8) from the lower Klimoli Formation of Inner Mongolia, North China.

Histiodella labiosa Bauer, 2010
Figures 3.1, 3.2, 4–6

?1979 *Histiodella* n. sp. Bergström, fig. 2C.
1979 *Histiodella* n. sp. 2 Harris et al., pl. 4, figs. 12, 13.
2010 *Histiodella labiosa* Bauer, p. 13, pl. 2, figs. 10, 11, 13, 14 (see for synonymy).
?2012 *Histiodella holodentata*; Stouge, part, fig. 9AA.
2020 *Histiodella labiosa*; Zhen and Rutledge, fig. 8a–c.
2021 *Histiodella labiosa*; Zhen, fig. 5n.
2021a *Histiodella labiosa*; Zhen et al., p. 273, fig. 12M.
2021b *Histiodella labiosa*; Zhen et al., fig. 5p.

Type series.—Lectotype (designated herein OSU 52034, originally figured by Bauer, 2010, pl. 2, fig. 13) and paralectotypes (OSU 52031 = M from sample 72SC-500; OSU 52032 = Sa from sample 72SC-470; OSU 52035 = Pb from sample 72SC-620, originally figured by Bauer, 2010, pl. 2, figs. 10, 11, 14, respectively).

Diagnosis.—Species of *Histiodella* consisting of carminate Pa and Pb elements, geniculate makellate M element, and ramiform S elements; Pa and Pb elements triangular in outline with a prominent cusp, a longer anterior process and with well-defined basal flange; Pa element with a narrow platform-like projection developed near mid-length

https://doi.org/10.1017/jpa.2022.26 Published online by Cambridge University Press

on the outer-lateral side, and confluent denticles on anterior and posterior processes; axes of the denticles on both processes parallel or sub-parallel to the axis of cusp; Pb element having a denticulate anterior process and a shorter posterior protoprocess with minutely serrated upper margin and a weakly developed platform-like projection on the outer-lateral side; M element typically with short denticles along inner-lateral margin (modified after Bauer, 2010, p. 13).

Description.—Species consisting of likely seximembrate apparatus of denticulate elements, including geniculate and typically denticulate makellate M, ramiform S (alate triform Sa, modified bipennate Sc, and possibly also including a modified tertiopedate Sb) and carminate Pa and Pb (both with a well-developed basal flange) elements. Carminate Pa element triangular in outline (H/L ratio varying from 0.52–0.86) with a prominent cusp and the denticulate anterior and posterior processes triangular in outline (Fig. 4); cusp suberect to weakly reclined, forming the apex of the element, laterally compressed and biconvex with sharp anterior and posterior edges, and width of three to four times as wide as the adjacent denticles in lateral view; anterior process longer, bearing 7–10 long, confluent denticles in full-growth specimens; posterior process slightly shorter, bearing 5–9 long, confluent denticles; cusp and denticles ornamented with fine striae; denticles on the two processes highest next to the cusp and progressively shorter distally; axes of denticles extending parallel or sub-parallel to the axis of cusp (more or less perpendicular to basal margin); platform-like projection prominent on the outer-lateral side, triangular in outline in apical view (Fig. 4.2, 4.8, 4.12); basal cavity shallow, slightly expanded underneath cusp and extending as a narrow groove to the distal end of the processes (Fig. 4.7).

Carminate Pb element shorter triangular in outline and shorter in length compared to the Pa (H/L ratio varying from 0.74–0.96) with a prominent cusp, a denticulate anterior process, and a shorter posterior protoprocess (Figs. 3.2, 5); cusp suberect to weakly reclined to form apex of the element, laterally compressed and biconvex with sharp anterior and posterior edges, and with a width of three to four times that of the adjacent denticles on the anterior process in lateral view; anterior process longer with a slightly convexly curved upper margin, bearing 4–9 long, confluent denticles that are highest next to the cusp and progressively shorter towards distal end; axes of denticles extending parallel or sub-parallel to axis of cusp; posterior margin of the cusp and upper margin of the posterior protoprocess extending smoothly into each other, straight (Fig. 5.5, 5.7) to slightly concavely curved (Fig. 5.6, 5.10) and minutely serrated in lateral view (Fig. 5.4); surface of cusp and denticles ornamented with fine striae; platform-like projection weakly developed on the outer-lateral side (Fig. 5.8).

Geniculate M element antero-posteriorly compressed with a robust and outer-laterally recurved cusp and a low, short base (Figs. 3.1, 6.2–6.9); cusp short and slightly bowed posteriorly, biconvex with sharp outer-lateral and inner-lateral margins, a more broadly convex anterior face and a broad carina on the posterior face (Fig. 6.2, 6.3, 6.5); inner-lateral margin gently curved and typically ornamented with 3–8 short denticles, less commonly denticles may be rudimentary (Bauer, 2010, pl. 2, fig. 10) or even absent; base expanding posteriorly to form a triangular outline in apical or basal view (Fig. 6.4) with a basal cavity of moderate depth (Fig. 6.2).

Ramiform S elements represented by alate triform Sa and modified bipennate Sc elements; Sa element bearing a denticulate blade-like lateral process on each side and sharp blade-like costa on the posterior face (Bauer, 2010, pl. 2, fig. 11); Sc element strongly compressed laterally and asymmetrical with a prominent cusp and an anterior process bearing five denticles (Fig. 6.1); cusp biconvex with sharp anterior and posterior margins.

Material illustrated.—Thirty topotypes (OSU 54951–54980), including Pa (11 specimens, Fig. 4) and Pb (10 specimens, Fig. 5), M (eight specimens, Fig. 6.2–6.9), and Sc (one specimen, Fig. 6.1) elements from the Oil Creek Formation, section 72SC, southern Oklahoma.

Remarks.—Bauer (2010) recognized carminate Pa and Pb elements, geniculate M, and ramiform Sa and Sb elements, but S elements are extremely rare with only eight specimens represented among a total of 997 specimens in his original study of *H. labiosa*. Reexamination of the current topotype material from sample 89JA-178 produced a single specimen representing the modified bipennate Sc (Fig. 6.1) of this species, supporting a possible seximembrate species apparatus for *H. labiosa*. However, Bauer (2010) included and described the Sb element as like alate Sa but with asymmetrically disposed lateral processes, but it was neither illustrated by him from the original type material nor recovered from the current samples of this study.

The Pa element of *H. labiosa* morphologically resembles that of *H. serrata* and *H. holodentata*, but differs from the latter two species by having a longer posterior process and by having denticles on the posterior process extending with their axes parallel or nearly parallel to the axis of the cusp. Bauer (2010) also noted the development of a narrow platform on the outer-lateral side of the Pa (Fig. 4.2, 4.8, 4.12) and Pb (Fig. 5.8) elements of *H. labiosa*—a distinctive character that has not been reported occurring in any other species of *Histiodella*.

Phylogeny and evolution of *Histiodella*

Although many species of *Histiodella* are cosmopolitan and widely used as biozonal index species for worldwide correlation of the upper Dapingian and lower to middle Darriwilian strata, their origin and evolution are still poorly understood. By including *H. donnae* as the most primitive species of *Histiodella*, Repetski and Repetski (2002) suggested that *Histiodella* might be directly evolved from a *Rossodus* species. Variable views exist to suggest that *Histiodella* evolved from an ancestral stock within Oistodontidae, but relating to different genera, including *Rossodus*, *Juanognathus*, *Tripodus*, *Protoprioniodus*, and *Cooperignathus*, by several authors (e.g., Ethington and Clark, 1982; Dzik, 1983; Sweet, 1988; Repetski and Repetski, 2002). Among these taxa considered to be the likely ancestor of *Histiodella*, only *Protoprioniodus* and *Cooperignathus*

https://doi.org/10.1017/jpa.2022.26 Published online by Cambridge University Press

have protopectiniform P elements in their species apparatuses, which share a number of the characters with the P elements of *Histiodella* species. To test these hypotheses, a phylogenetic analysis was conducted in this study by selecting *Cooperignathus nyinti* as the outgroup, which resulted in a well-resolved hierarchical clustering that infers the evolutionary relationship of all the 10 confirmed species of *Histiodella* (Figs. 7–9). *Rossodus*, *Juanognathus*, and *Histiodella donnae* are less closely related to *Histiodella*. Having coniform P elements (in *Rossodus*) or lacking P elements (in *Juanognathus* and *Histiodella donnae*) in their species reconstructions prevents a direct morphological comparison with the protopectiniform or pectiniform Pa elements of the *Histiodella* species. *Tripodus* species have the protopastinate P elements in their species apparatuses (Sweet, 1988, fig. 5.12), which suggests a closer affinity with Prioniodontidae. Therefore, these taxa have been excluded from the analysis conducted herein.

Our analysis shows a closer relationship between *Histiodella* and *Cooperignathus* of the Early Ordovician. The protoanguliplanate P elements of *Cooperignathus* (Fig. 3.4) may represent the earliest geological record of true pectiniform elements that have several shared synapomorphies with *Histiodella* species, including the occurrence of a basal flange and basal surface (Fig. 7). Both *Cooperignathus nyinti* and *C. aranda* also have a narrow platform-like projection on the outer-lateral face of the P elements (Zhen et al., 2003, in press), which is comparable with that developed on the outer-lateral face of the Pa element of *H. labiosa* (Fig. 4.2, 4.8, 4.12).

Based on the morphometric analysis of the *Histiodella* species recovered from the Joins Formation of the Arbuckle Mountains of Oklahoma, McHargue (1982) established two evolutionary trends, namely (1) evolving from adentate early species (*H. altifrons*) to partially denticulate (e.g., *H. sinuosa* with only anterior process) and then to fully denticulate (e.g., *H. serrata* and *H. labiosa* with anterior and posterior processes), and (2) from a relatively high blade morphology in the early species (e.g., *H. altifrons* and *H. minutiserrata*) to more elongated shape of the late species (e.g., *H. bellburnensis*) by decreasing height/length ratio of the Pa elements. Our current study of the morphology and their stratigraphic ranges of the 10 *Histiodella* species also shows that the general shape of their Pa elements has evolved from a triangular outline of the early species (e.g., *H. altifrons*, *H. minutiserrata*, *H. sinuosa*, and *H. labiosa*) to a more or less rectangular form of the late species (e.g., *H. kristinae* and *H. bellburnensis*; Fig. 7). The apex of the Pa elements also changed from a location towards posterior in the early species (e.g., *H. altifrons* and *H. minutiserrata*) to more or less centrally positioned (*H. labiosa*) and then to anteriorly positioned in the late species (e.g., *H. kristinae* and *H. bellburnensis*). The cusp evolved from robust and high in the early species to inconspicuous in the late species (Fig. 7).

Cladistic analysis.—To test the validity of these inferred phylogenetic relationships, the 10 species of *Histiodella*, plus *Cooperignathus nyinti* acting as the outgroup, were scored using the following 12 binary characters of the Pa elements and were then cladistically analyzed by applying reductive coding strategy (Table 1).

Table 1. Data matrix for the 10 species of *Histiodella* and outgroup, *Cooperignathus nyinti* (Cooper, 1981) (composite coding, with 12 binary characters, N = inapplicable). See text for descriptions of characters 1–12.

Characters	1	2	3	4	5	6	7	8	9	10	11	12
Cooperignathus nyinti	1	1	0	0	0	0	N	N	N	N	N	N
Histiodella altifrons	1	1	1	0	0	0	N	N	0	0	0	0
Histiodella minutiserrata	1	1	1	1	0	0	N	N	0	0	0	0
Histiodella sinuosa	1	1	1	1	1	0	0	N	0	0	0	0
Histiodella labiosa	1	1	1	1	1	1	1	0	0	0	0	0
Histiodella serrata	1	1	1	1	1	1	0	1	0	0	0	0
Histiodella holodentata	1	1	1	1	1	1	0	1	1	0	0	0
Histiodella kristinae	1	1	1	1	1	1	0	1	1	1	0	0
Histiodella wuhaiensis	1	1	1	1	1	1	0	1	1	1	1	0
Histiodella bellburnensis	1	1	1	1	1	1	0	1	1	1	1	0
Histiodella triangularis	1	1	1	1	1	1	0	1	1	1	1	1

Character 1.—Basal flange and basal surface: absent (0), present (1). All 10 species of *Histiodella* and the out-group are coded as (1).

Character 2.—Protopectiniform or pectiniform: absent (0), present (1). All 10 species of *Histiodella* and the out-group are coded as (1).

Character 3.—Presence of cusp: absent (0), present (1). This is a character shared by all 10 species of *Histiodella*, with *C. nyinti* coded as (0).

Character 4.—Denticulated or serrated: absent (0), present (1). This is a character shared by nine species of *Histiodella* that are coded as (1), with *H. altifrons* and *C. nyinti* coded as (0).

Character 5.—Denticles on anterior process: absent (0), present (1). This is a character shared by eight species of *Histiodella* that are coded as (1), with *H. minutiserrata*, *H. altifrons*, and *C. nyinti* coded as (0).

Character 6.—Denticle on posterior process: absent (0), present (1). This character is shared by seven species of *Histiodella* that are coded as (1), with *H. sinuosa*, *H. minutiserrata*, *H. altifrons*, and *C. nyinti* coded as (0).

Character 7.—Axes of denticles on posterior process parallel to axis of the cusp: absent (0), present (1). This character features *H. labiosa* coded as (1). It is inapplicable for *H. minutiserrata*, *H. altifrons*, and *C. nyinti*, which are coded as (N). Others are coded as (0).

Character 8.—Reclined denticles on posterior process: absent (0), present (1). This character is shared by six species of *Histiodella* that are coded as (1), with *H. labiosa* coded as (0). It is inapplicable for *H. sinuosa*, *H. minutiserrata*, *H. altifrons*, and *C. nyinti*, which are coded as (N).

Character 9.—Rectangular outline in lateral view: absent (0), present (1). This character is shared by five species of *Histiodella* that are coded as (1), with the other five species of *Histiodella* coded as (0). It is inapplicable for *C. nyinti*, which is coded as (N).

Character 10.—Apex of the unit is located toward anterior end: absent (0), present (1). This character is shared by four species of *Histiodella* that are coded as (1), with the other six species of *Histiodella* coded as (0). It is inapplicable for *C. nyinti*, which is coded as (N).

Character 11.—Small or inconspicuous cusp: absent (0), present (1). This character is shared by three species of *Histiodella* that are coded as (1), with the other seven species of *Histiodella* coded as (0). It is inapplicable for *C. nyinti*, which is coded as (N).

https://doi.org/10.1017/jpa.2022.26 Published online by Cambridge University Press

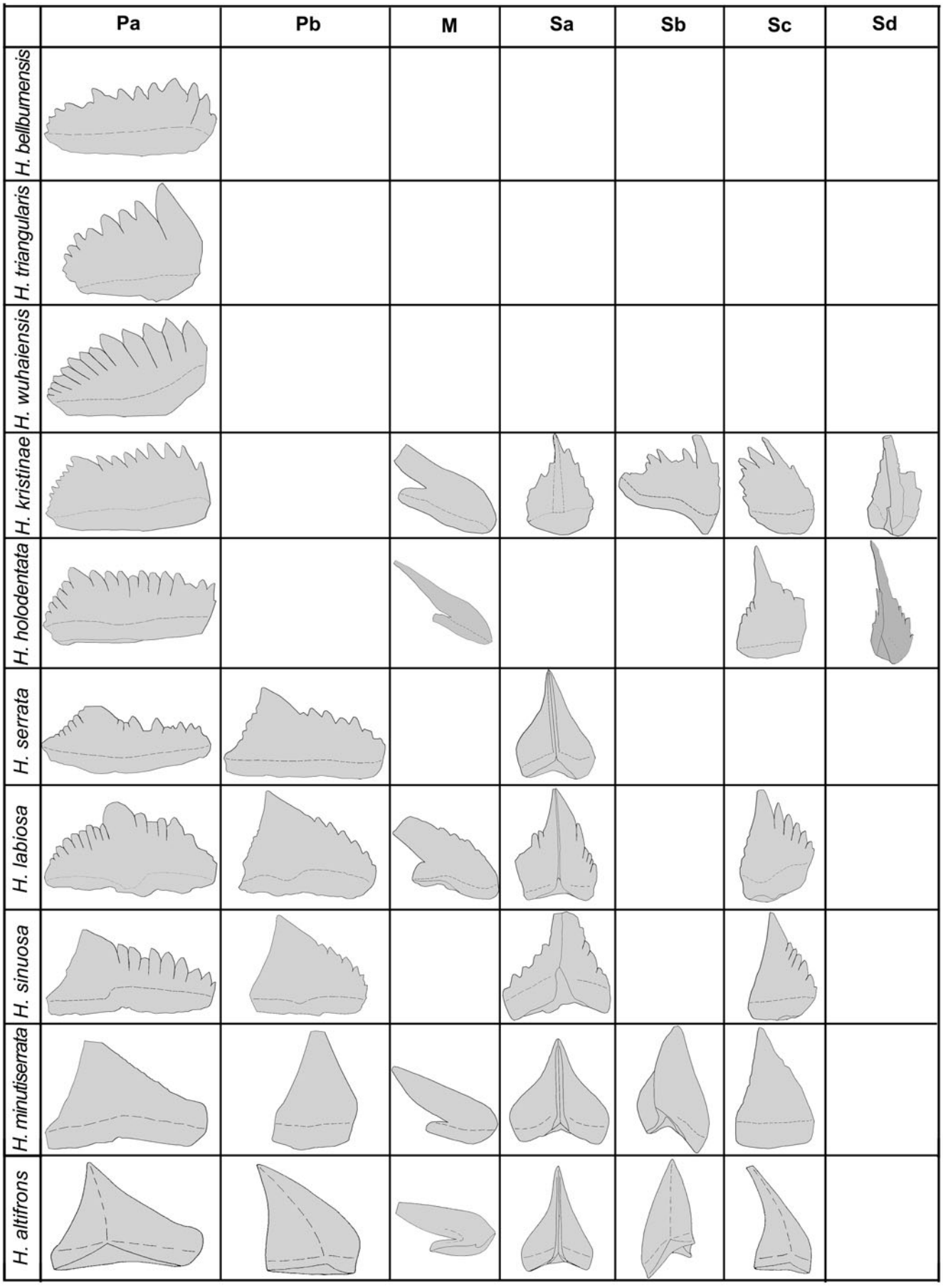

https://doi.org/10.1017/jpa.2022.26 Published online by Cambridge University Press

Figure 7. Species apparatus and comparison of the constituent elements of the 10 *Histiodella* species (sources of data from Harris, 1962; Mound, 1965; Ethington and Clark, 1982; McHargue, 1982; Stouge, 1984, 2012; Wang and Lou, 1984; Bauer, 2010; Wang et al., 2013; this study).

Character 12.—Strongly reduced anterior process: absent (0), present (1). This character features in *H. triangularis*, which is coded as (1), with other species of *Histiodella* coded as (0). It is inapplicable for *C. nyinti*, which is coded as (N).

Histiodella *cladogram.*—The cladogram produced is highly resolved (Fig. 8). It depicts the origin of this biostratigraphically valuable genus in the Middle Ordovician and its close phylogenetic affinity with late Floian (Early Ordovician) *Cooperignathus*, suggesting that both genera might share a common adentate ancestor (within Oistodontidae). It also supports the monophyletic grouping of the 10 *Histiodella* species and the evolutionary trends that have been revealed from the analyses of morphological changes and morphometrics among these species (e.g., McHargue, 1982; Feltes and Albanesi, 2017). Our study is consistent with the results derived from the geometric morphometric analysis of five *Histiodella* species conducted by Feltes and Albanesi (2017), demonstrating that the *Histiodella* species evolved through continuous changes in shape of the element outlines and size and height of denticles of the Pa elements.

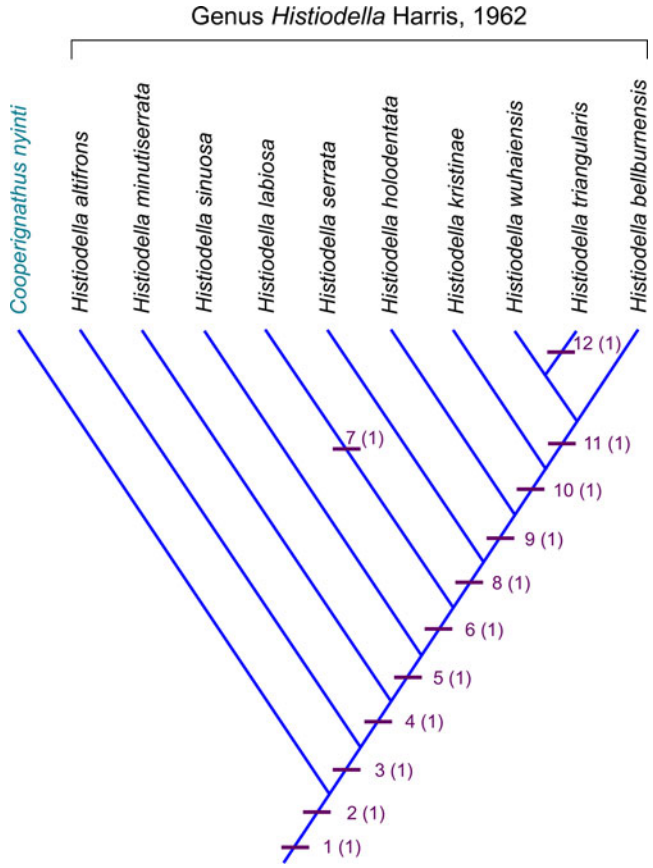

Figure 8. Cladogram showing the inferred phylogenetic relationships of the 10 *Histiodella* species by using data analysis program PAST (as unweighted and unordered; Algorithm: Branch-and-bound; Optimization: Wagner) with *Cooperignathus nyinti* (Cooper, 1981) as the outgroup; dataset coded with 12 binary characters of the Pa elements (see text for description).

Distribution and biostratigraphy

With their distinctive morphology and short stratigraphic ranges, *Histiodella* species are recognized as excellent markers in subdivision and correlation of the lower and middle Darriwilian strata (Fig. 9). Occurrence of the six *Histiodella* species in the Joins and Oil Creek formations exposed in southern Oklahoma represents the best record of these species worldwide. Five conodont biozones are defined, with the *H. altifrons* Biozone recognized in the lower part of the Joins Formation (Figs. 2, 9). The succeeding *H. minutiserrata* Biozone is marked by the FAD (First Appearance Datum) of the eponymous species as the base and the FAD of *H. sinuosa* as the top (Figs. 2, 9). As the primitive forms of *Histiodella*, *H. altifrons* is the only adentate species and *H. minutiserrata*, which is characterized by having minutely serrated upper margin of the Pa element, might be directly evolved from it. Apart from their wide distribution in North America (e.g., Harris, 1962; Mound, 1965; Bradshaw, 1969; Harris et al., 1979; Ethington and Clark, 1982; McHargue, 1982; Norford et al., 2002; Bauer, 2010), these two species are generally found as minor faunal components in the Argentine Precordillera (Lehnert, 1995; Albanesi et al., 2006; Voldman et al., 2015), central Asian Fold Belt (Tolmacheva, 2014, referred to as *Histiodella* cf. *H. altifrons* and *Histiodella* sp. 1, respectively), and Australia (Nicoll, 1992, 1993; Zhen et al., 2020a, b). The eponymous species of the *H. sinuosa* Biozone is the oldest species of *Histiodella* bearing true denticles (but only on the anterior process, Fig. 7). This biozone is utilized to correlate lower Darriwilian strata in Laurentia (Fig. 9), and is recognized in the Argentine Precordillera (e.g., Carrera et al., 2013; Serra et al., 2015, 2019, 2020; Feltes et al., 2016) and central Asian Fold Belt (Tolmacheva, 2014).

Bauer (2010) established the *H. labiosa* Biozone based on the appearance of *H. labiosa* and its stratigraphic range in the Oil Creek Formation within the section 72SC in southern Oklahoma. It was confined by the FAD of the eponymous species as the base and the FAD of *H. holodentata* as the top. *Histiodella labiosa* first occurs in sample 72SC-40 at a horizon 12.19 m above the base of the Oil Creek Formation (Bauer, 2010, table 1) and extends to the top of the Oil Creek Formation. *Histiodella holodentata* is very rare in the Oil Creek Formation at section 72SC. Bauer (2010, pl. 2, fig. 9; Fig. 2) illustrated a specimen representing the Pa element of *H. holodentata* recovered from sample 72SC-620 (at a horizon 188.98 m above the base of the Oil Creek Formation). Two additional specimens representing the Pa element of this species were also recovered from sample 72SC-440 (at a horizon 134.11 m above the base of the Oil Creek Formation). Therefore, the boundary between the *H. holodentata*/*H. labiosa* biozones in section 72SC is drawn in the middle of the Oil Creek Formation, 134.11 m above the base of the Oil Creek Formation (Fig. 2). Abundant *H. labiosa* and rare *H. holodentata* in the upper Oil Creek Formation suggested that two species might have favored different habitats. Distribution of *H. labiosa* in North America was detailed by Bauer (2010), and the synonym list in this study also includes a recent

https://doi.org/10.1017/jpa.2022.26 Published online by Cambridge University Press

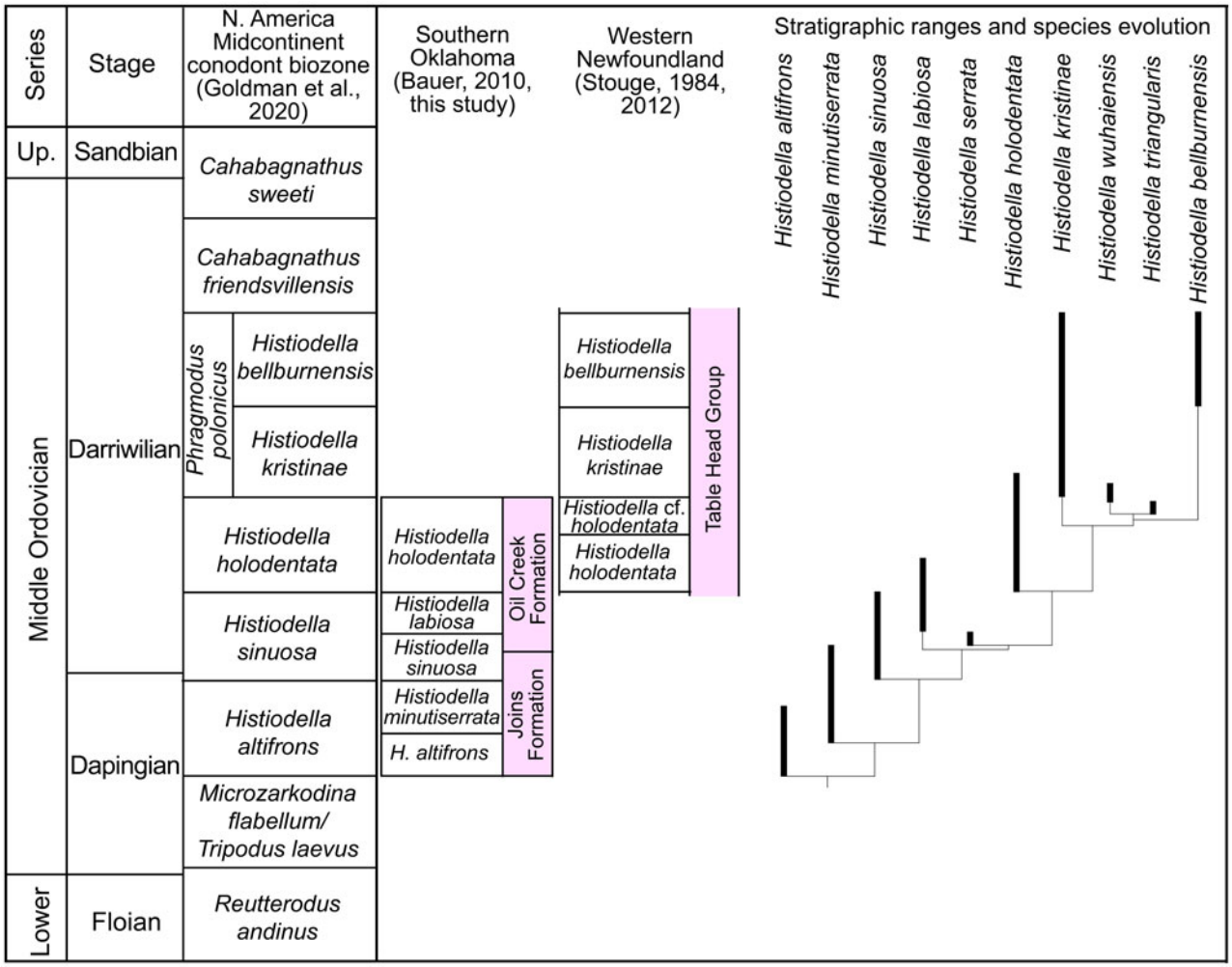

Figure 9. Stratigraphic ranges of the 10 *Histiodella* species and their inferred species evolution. Up. = Upper Ordovician; Lower = Lower Ordovician.

report of this species from the top part of the Willara Formation in the Canning Basin of Western Australia (Zhen et al., 2021a) and from the chert beds within the Abercrombie Formation of the turbiditic sequences in New South Wales (Zhen and Rutledge, 2020; Zhen, 2021; Zhen et al., 2021b). Occurrence of this species from two separate paleobiogeographic domains in the Ordovician tropical zone (Laurentia and eastern Gondwana) indicates that *H. labiosa* may have a wide geographical distribution and be potentially useful for correlation of the lower Darriwilian Stage worldwide.

Histiodella serrata, *H. holodentata*, and *H. kristinae* are cosmopolitan, with wider distribution geographically than other species of *Histiodella*, and have played an important role in the detailed biostratigraphic correlation of early and middle Darriwilian worldwide (Bergström and Ferretti, 2017; Goldman et al., 2020; Zhen, 2021). Continuous succession consisting of the *H. holodentata*, *H. kristinae*, and *H. bellburnensis* biozones were well recorded from the Table Head Group of Newfoundland (Stouge, 1984, 2012; Fig. 9). Apart from their wide occurrence in North America, *H. holodentata* and *H. kristinae* also occur in the Argentine Precordillera (e.g., Albanesi, 1998; Albanesi and Ortega, 2003, 2016; Mestre, 2012; Serra et al., 2015, 2017, 2019, 2020; Feltes et al., 2016), Australasia (e.g., Zhen and Percival, 2004; Zhen et al., 2009, 2020a, 2021b; Zhen and Rutledge, 2020), major Chinese terranes (e.g., An and Zheng, 1990; Du et al., 2005; Wang et al., 2011; Zhen et al., 2011, 2020b), southern Asia (Agematsu et al., 2006, 2008), the central Asian Fold Belt (e.g., Tolmacheva, 2014), and Baltoscandia (e.g., Rasmussen, 2001; Löfgren, 2004; Viira, 2011). The *H. holodentata* and *H. kristinae* biozones of the middle Darriwilian (= Dw2 stage slice of Bergström et al., 2009) now can be correlated precisely across shallow-water carbonate platform to deep-water slope settings, and well integrated with graptolite successions (Maletz, 2009; Stouge, 2012). *Histiodella bellburnensis*, representing one of the most derived forms of the genus, also has been reported from the Tarim Basin (Du et al., 2005), North China (Jing et al., 2020), and the Argentine Precordillera (Serra et al., 2015, 2019). *Histiodella triangularis* and *H. wuhaiensis*, representing the two other most-derived forms, originally were reported from North China and recently were recorded from Australia (Zhen, 2021).

Conclusions

With formal designation of a lectotype, a revised diagnosis, detailed description, and morphological comparisons with its

https://doi.org/10.1017/jpa.2022.26 Published online by Cambridge University Press

direct ancestor and descendant, *Histiodella labiosa* Bauer, 2010, is now accepted as a valid species, which is morphologically distinctive and biostratigraphically valuable for correlation of the lower Darriwilian Stage. Analysis of the morphological changes among the 10 known species of *Histiodella* has revealed that *Histiodella* species evolved through continuous changes in shape of element outlines, size and height of denticles, and cusp size and position of the Pa elements. The phylogenetic and morphometric analysis conducted in this study indicates that the 10 known species of *Histiodella* represent a monophyletic group, which is especially important to support the wide use of these species in subdividing and correlating late Dapingian to middle Darriwilian strata worldwide.

Acknowledgments

Research of the senior author was supported by the Geological Survey of New South Wales. P. Carter (Geological Survey of New South Wales) assisted with the final drafting of Figure 1. SEM images were prepared in the Electron Microscope Unit of Macquarie University with assistance from S. Lindsay. J. Repetski and G. Albanesi are thanked for their careful and constructive reviews of the manuscript. Y. Y. Zhen publishes with permission of the Executive Director, Geological Survey of New South Wales. This is a contribution to IGCP Project 735 (Rocks and the Rise of Ordovician Life) and IGCP Project 668 (Equatorial Gondwana History and Early Paleozoic Evolutionary Dynamics).

Disclosure statement

No potential conflict of interest was reported by the authors.

References

Agematsu, S., Sashida, K., Salyapongse, S., and Sardsud, A., 2006, Ordovician conodonts from the Thong Pha Phum area, western Thailand: Journal of Asian Earth Sciences, v. 26, p. 49–60.

Agematsu, S., Sashida, K., and Sardsud, A., 2008, Reinterpretation of Early and Middle Ordovician conodonts from the Thong Pha Phum area, western Thailand, in the context of new material from western and northern Thailand: Paleontological Research, v. 12, p. 181–194.

Albanesi, G., 1998, Taxonomía de conodontes de las secuencias ordovícicas del Cerro Potrerillo, Precordillera Central de San Juan, República Argentina: Actas, Academia Nacional de Ciencias de Córdoba, v. 12, p. 99–253.

Albanesi, G.L., and Ortega, G., 2003, Advances on conodont-graptolite biostratigraphy of the Ordovician System of Argentina, *in* Aceñolaza, F.G. ed., Aspects of the Ordovician System of Argentina: Tucumán, INSUGEO, Serie Correlación Geológica, v. 16, p. 143–165.

Albanesi, G.L., and Ortega, G., 2016, Conodont and graptolite biostratigraphy of the Ordovician System of Argentina: *in* Montenari, M., ed., Stratigraphy and Timescales: Cambridge, Elsevier Inc, Academic Press, p. 61–121.

Albanesi, G.L., Carrera, M.G., Cañas, F.L., and Saltzman, M., 2006, A proposed global boundary stratotype section and point (GSSP) for the base of the Middle Ordovician Series: the Niquivil section, Precordillera of San Juan, Argentina: Episodes, v. 29, p. 1–15.

An, T.X., 1987, Early Palaeozoic Conodonts from South China: Beijing, Peking University Publishing House, 238 p. [in Chinese with English abstract]

An, T.X., and Zheng, S.C., 1990, The Conodonts of the Marginal Areas Around the Ordos Basin, North China: Beijing, Science Press, 199 p. [in Chinese with English abstract]

An, T.X., Du, G.Q., Gao, Q.Q., Chen, X.B., and Li, W.T., 1981, Ordovician conodont biostratigraphy of the Huanghuachang area of Yichang, Hubei, *in* Micropalaeontological Society of China, ed., Selected Papers of the First Symposium of the Micropalaeontological Society of China: Beijing, Science Press, p. 105–113. [in Chinese]

An, T.X., Zhang, F., Xiang, W.D., Zhang, Y.Q., Xu, W.H., Zhang, H.J., Jiang, D.B., Yang, C.S., Lin, L.D., Cui, Z.T., and Yang, X.C., 1983, The Conodonts of North China and the Adjacent Regions: Beijing, Science Press, 223 p. [in Chinese with English abstract]

An, T.X., Du, G.Q., and Gao, Q.Q., 1985, Ordovician Conodonts from Hubei: Beijing, Geological Publishing House, 64 p. [in Chinese with English abstract]

Bauer, J.A., 2010, Conodonts and conodont biostratigraphy of the Joins and Oil Creek formations, Arbuckle Mountains, south-central Oklahoma: Oklahoma Geological Survey Bulletin, v. 150, p. 1–44.

Bergström, S.M., 1979, Whiterockian (Ordovician) conodonts from the Hølonda Limestone of the Trondheim Region, Norwegian Caledonides: Norsk Geologisk Tidsskrift, v 59, p. 295–307.

Bergström, S.M., and Ferretti, A., 2017, Conodonts in Ordovician biostratigraphy: Lethaia, v. 50, p. 424–439.

Bergström, S.M., Chen, X., Gutiérrez-Marco, J.C., and Dronov, A., 2009, The New chronostratigraphic classification of the Ordovician System and its relations to major regional series and stages and to $\delta^{13}C$ chemostratigraphy: Lethaia, v. 42, p. 97–107.

Bradshaw, L.E., 1969, Conodonts from the Fort Peña Formation (Middle Ordovician), Marathon Basin, Texas: Journal of Paleontology, v. 43, p. 1137–1168.

Carlucci, J.R., Goldman, D., Brett, C.E., Westrop, S.R., and Leslie, S.A., 2015, Katian GSSP and carbonates of the Simpson and Arbuckle groups in Oklahoma: Stratigraphy, v. 2, p. 144–202.

Carrera, M.G., Fenoglio, F., Albanesi, G.L., and Voldman, G., 2013, Conodonts, sequence stratigraphy and the drowning of the San Juan carbonate platform in the Ordovician of the Argentine Precordillera: *in* Albanesi, G.L., and Ortega, G. eds., Conodonts from the Andes. Proceedings of the 3rd International Conodont Symposium & Regional Field Meeting of the IGCP project 591: Asociación Paleontológica Argentina, Publicación Especial, no. 13, p. 5–12.

Clark, D.L., Sweet, W.C., Bergström, S.M., Klapper, G., Austin, R.L., Rhodes, F.H.T., Müller, K.J., Ziegler, W., Lindström, M., Miller, J.F., and Harris, A.G., 1981, Conodonta, *in* Robison, R.A., ed., Treatise on Invertebrate Paleontology, part W, Miscellanea, supplement 2:, Boulder, Colorado, and Lawrence, Kansas, Geological Society of America and University of Kansas, 202 p.

Cooper, B.J., 1981, Early Ordovician conodonts from the Horn Valley Siltstone, central Australia: Palaeontology, v. 24, p. 147–183.

Decker, C.E., and Merritt, C.A., 1931, The stratigraphy and physical characteristics of the Simpson Group: Oklahoma Geological Survey Bulletin 55, 112 p.

Derby, J.R., Bauer, J.A., Creath, W.B., Dresbach, R.I., Ethington, R.L., Loch, J.D., Stitt, J.H., McHargue, T.R., Miller, J.F., Miller, M.A., and Repetski, J.E., 1991, Biostratigraphy of the Timbered Hills, Arbuckle, and Simpson groups, Cambrian and Ordovician, Oklahoma: a review of correlation tools and techniques available to the explorationist: Oklahoma Geological Survey Circular, v. 92, p. 15–41.

Du, P.D., Zhao, Z.X., Huang, Z.B., Tan, Z.J., Wang, C., Yang, Z.L., Zhang, G.Z., and Xiao, J.N., 2005, Discussion on four conodont species of *Histiodella* from Tarim Basin and their stratigraphic implication: Acta Micropalaeontologica Sinica, v. 22, p. 357–369. [in Chinese with English abstract]

Dzik, J., 1976, Remarks on the evolution of Ordovician conodonts: Acta Palaeontologica Polonica, v. 21, p. 395–455.

Dzik, J., 1983, Relationships between Ordovician Baltic and North American Midcontinent conodont faunas: Fossils and Strata, v. 15, p. 59–85.

Dzik, J., 1991, Evolution of oral apparatuses in the conodont chordates: Acta Palaeontologia Polonica, v. 36, p. 265–323.

Ethington, R.L., and Clark, D.L., 1982, Lower and Middle Ordovician conodonts from the Ibex area, western Millard County, Utah: Brigham Young University, Geological Studies 28, p. 1–160.

Ethington, R.L., Repetski, J.E., and Derby, J. R., 2012, Ordovician of the Sauk megasequence in the Ozark region of northern Arkansas and parts of Missouri and adjacent States: *in* Derby, J.R., Fritz, R.D., Longacre, S.A., Morgan, W.A., and Sternbach, C.A. eds., The Great American Carbonate Bank: The Geology and Economic Resources of the Cambrian–Ordovician Sauk Megasequence of Laurentia: AAPG Memoir, v. 98, p. 275–300.

Ettensohn, F.R., Pashin, J.C., and Gilliam, W., 2019, The Appalachian and Black Warrior basins: foreland basins in the eastern United States: *in* Miall, A.D., ed., The Sedimentary Basins of the United States and Canada (Second Edition): Sedimentary Basins of the World: Amsterdam, Elsevier, p. 129–237.

Feltes, N.A., and Albanesi, G.L., 2017. Directional evolution in the *Histiodella* lineage: *in* Liao, J-C., and Valenzuela-Rios, J.I., eds., Fourth International Conodont Symposium. ICOS IV "Progress on Conodont Investigation": Cuadernos del Museo Geominero, no. 22, p. 283–288.

Feltes, N.A., Albanesi, G.L., and Bergström, S.M., 2016, Conodont biostratigraphy and global correlation of the middle Darriwilian–lower Sandbian Las

https://doi.org/10.1017/jpa.2022.26 Published online by Cambridge University Press

Aguaditas Formation, Precordillera of San Juan, Argentina: Andean Geology, v. 43, p. 60–85.
Goldman, D., Sadler, P.M., and Leslie, S.A., 2020, Chapter 20—The Ordovician Period: *in* Gradstein, F.M., Ogg, J.G., Schmitz, M.D., and Ogg, G.M., eds., Geologic Time Scale: Amsterdam, Elsevier B.V., p. 631–694.
Graves, R.W., and Ellison, S., 1941, Ordovician conodonts of the Marathon Basin, Texas: University of Missouri, School of Mines and Metallurgy, Bulletin of the Technical Series 14, 26 p.
Ham, W.E., 1973, Regional geology of the Arbuckle Mountains, Oklahoma: Oklahoma Geological Survey Special Publication 73-3, 61 p.
Harris, A.G., Bergström, S.M., Ethington, R.L., and Ross, R.J., Jr., 1979, Aspects of Middle and Upper Ordovician conodont biostratigraphy of carbonate facies in Nevada and southeast California and comparison with some Appalachian successions: Brigham Young University Geology Studies, v. 26, no. 3, p. 7–44.
Harris, R.W., 1962, New conodonts from Joins (Ordovician) Formation of Oklahoma: Oklahoma Geology Notes 22, p. 199–211.
Henry, M.E., 1988, Review of the geology of the southern Oklahoma fold belt province as a basis for estimates of undiscovered hydrocarbon resources: U.S. Geological Survey, Open-File Report 87-450W, p. 1–21.
Jing, X.C., Zhou, H.R., Wang, X.L., Yang, Z.H., Fang, Q., Wang, Z.T., and Fan, J., 2020, A review on Ordovician conodont biostratigraphy of the North China Plate and new research advances on its northwestern margin: Earth Science Frontiers, v. 27, p. 199–212.
Lehnert, O., 1995, Ordovizische Conodonten aus der Präkordillere Westargentiniens: Ihre Bedeutung für Stratigraphie und Paläogeographie: Erlanger Geologische Abhandlungen, v. 125, p. 1–193.
Lindström, M., 1970, A suprageneric classification of the conodonts: Lethaia, v. 3, p. 427–445.
Löfgren, A., 2004, The conodont fauna in the Middle Ordovician *Eoplacognathus pseudoplanus* Zone of Baltoscandia: Geological Magazine, v. 141, p. 505–524.
Maletz, J., 2009, *Holmograptus spinosus* and the Middle Ordovician (Darriwilian) graptolite biostratigraphy at Les Méchins (Quebec, Canada): Canadian Journal of Earth Sciences, v. 46, p. 739–755.
McHargue, T.R., 1975, Conodonts of the Joins Formation (Ordovician), Arbuckle Mountains, Oklahoma [M.A. thesis]: Columbia, Missouri, University of Missouri, 151 p.
McHargue, T.R., 1982, Ontogeny, phylogeny, and apparatus reconstruction of the conodont genus *Histiodella*, Joins Fm., Arbuckle Mountains, Oklahoma: Journal of Paleontology, v. 56, p. 1410–1433.
Mestre, A., 2012, Bioestratigrafía de conodontes del techo de la Formación San Juan y el miembro inferior de la Formación Los Azules, Cerro La Chilca, Precordillera Central: Ameghiniana, v. 49, p. 185–197.
Morgan, W.A., 2012, Sequence stratigraphy of the Great American Carbonate Bank, chapter 4: *in* Derby, J.R., Fritz, R.D., Longacre, S.A., Morgan, W.A., and Sternbach, C.A. eds., The Great American Carbonate Bank: The Geology and Economic Resources of the Cambrian–Ordovician Sauk Megasequence of Laurentia: AAPG Memoir 98, p. 37–82.
Moskalenko, T.A., 1982, Conodonts, *in* Sokolov, B.S., ed., The Ordovician of the Siberian Platform. Key Section on the Kulumbe River: Moscow, Nauka, p. 100–144, 182–190.
Moskalenko, T.A., 1983, Conodonts and biostratigraphy in the Ordovician of the Siberian Platform: Fossils and Strata, v. 15, p. 87–94.
Mound, M.C., 1965, A conodont fauna from the Joins Formation (Ordovician), Oklahoma: Tulane Studies in Geology, v. 4, p. 1–46.
Nicoll, R.S., 1990, The genus *Cordylodus* and a latest Cambrian–earliest Ordovician conodont biostratigraphy: BMR Journal of Australian Geology and Geophysics, v. 11, p. 529–558.
Nicoll, R.S., 1992, Analysis of conodont apparatus organization and the genus *Jumudontus* (Conodonta), a coniform-pectiniform apparatus structure from the Early Ordovician: BMR Journal of Australian Geology and Geophysics, v. 13, p. 213–228.
Nicoll, R.S., 1993, Ordovician conodont distribution in selected petroleum exploration wells, Canning Basin, Western Australia: Australian Geological Survey Organisation, Record 1993/17, p. 1–136.
Norford, B.S., Jackson, D.E., and Nowlan, G.S., 2002, Ordovician stratigraphy and faunas of the Glenogle Formation, southeastern British Columbia: Geological Survey of Canada Bulletin, v. 569, p. 1–83.
Pander, C.H., 1856, Monographie der fossilen Fische des Silurischen Systems der Russisch-Baltischen Gouvernements: St. Petersburg, Akademie der Wissenschaften, 91 p.
Rasmussen, J. A., 2001, Conodont biostratigraphy and taxonomy of the Ordovician shelf margin deposits in the Scandinavian Caledonides: Fossils and Strata, v. 48, p. 1–180.
Read, J.F., and Repetski, J.E., 2012, Cambrian–lower Middle Ordovician passive carbonate margin, southern Appalachians: *in* Derby, J.R., Fritz, R.D., Longacre, S.A., Morgan, W.A., and Sternbach, C.A. eds., The Great American Carbonate Bank: The Geology and Economic Resources of the Cambrian–Ordovician Sauk Megasequence of Laurentia: AAPG Memoir, v. 98, p. 357–382.
Repetski, J.E., 1982, Conodonts from E1 Paso Group (Lower Ordovician) of westernmost Texas and southern New Mexico: New Mexico Bureau of Mines and Mineral Resources, Memoir, v. 40, p. 1–121.
Repetski, J.E., and Ethington, R.L., 1983, *Rossodus manitouensis* (Conodonta), a new Early Ordovician index fossil: Journal of Paleontology, v. 57, p. 289–301.
Repetski, J.E., and Repetski, R., 2002, The apparatus of *Histiodella donnae* and its phylogenetic relationships: Eighth International Conodont Symposium, Toulouse-Albi, June 22–25, 2002, Abstracts, Strata, Série 1, v. 12, p. 101.
Repetski, J.E., Loch, J.D., and Ethington, R.L., 1998, Conodonts and biostratigraphy of the Lower Ordovician Roubidoux Formation in and near the Ozark National Scenic Riverways, southeastern Missouri, *in* Santucci, V.L., and McClelland, L., eds., National Park Service Paleontological Research: Geologic Resources Division Technical Report NPS/NRGRD/GRDTR-98/01, p. 109–115.
Serra, F., Albanesi, G.L., Ortega, G., and Bergström, S.M., 2015, Conodont-graptolite biostratigraphy and global correlation of the mid-Late Ordovician in the Las Chacritas River section, Precordillera of San Juan, Argentina: Geological Magazine, v. 152, p. 813–829.
Serra, F., Feltes, N.A., Henderson, M.A., and Albanesi, G.L., 2017, Paleoecology of Darriwilian conodonts from the Central Precordillera of Argentina: Marine Micropaleontology, v. 130, p. 15–28.
Serra, F., Feltes, N.A., Albanesi, G.L., and Goldman, D., 2019, High-resolution conodont biostratigraphy from the Darriwilian Stage (Middle Ordovician) of the Argentine Precordillera and biodiversity analyses: a CONOP9 approach: Lethaia, v. 52, p. 188–203.
Serra, F., Feltes, N.A., Mango, M., Henderson, M.A., Albanesi, G.L., and Ortega, G., 2020, Darriwilian (Middle Ordovician) conodonts and graptolites from the Cerro La Chilca Section, Central Precordillera, Argentina: Andean Geology, v. 47, p. 125–143.
Stouge, S., 1984, Conodonts of the Middle Ordovician Table Head Formation, western Newfoundland: Fossils and Strata, v. 16, p. 1–145.
Stouge, S., 2012, Middle Ordovician (late Dapingian–Darriwilian) conodonts from the Cow Head Group and Lower Head Formation, western Newfoundland, Canada: Canadian Journal of Earth Sciences, v. 49, p. 59–90.
Sweet, W.C., 1988, The Conodonta: Morphology, Taxonomy, Paleoecology, and Evolutionary History of a Long-Extinct Animal Phylum: Oxford, Clarendon Press, 212 p.
Sweet, W.C., Ethington, R.L., and Harris, A.G., 2005, A conodont-based standard reference section in central Nevada for the lower Middle Ordovician Whiterockian Series: Bulletins of American Paleontology, v. 369, p. 35–52.
Taylor, J.F., Repetski, J.E., Loch, J.D., and Leslie, S.A., 2012, Biostratigraphy and chronostratigraphy of the Cambrian–Ordovician Great American Carbonate Bank, Chapter 3, *in* Derby, J.R., Fritz, R.D., Longacre, S.A., Morgan, W.A., and Sternbach, C.A., eds., The Great American Carbonate Bank: The Geology and Economic Resources of the Cambrian–Ordovician Sauk Megasequence of Laurentia: AAPG Memoir, v. 98, p. 15–36.
Thomas, W.A., 1991, The Appalachian-Ouachita rifted margin of southeastern North America: Geological Society of America Bulletin, v. 103, p. 415–431.
Tolmacheva, T.Yu., 2014, Biostratigraphy and biogeography of Ordovician conodonts from the western part of the Central Asian Fold Belt: Trudy VSEGEI, Novayaseriya, v. 356, p. 1–264. [in Russian]
Tolmacheva, T. Yu., Dronov, A.V., Alekseev, A.S., Danukalova, M.K., and Larionov, A.N., 2019, Biogeography of Ordovician conodonts in the Russian arctic and its implication for paleogeography, *in* Obut, O.T., Sennikov, N.V., and Kipriyanova, T.P., eds, Thirteenth International Symposium on the Ordovician System—Contributions of International Symposium. Novosibirsk, Russia (July 19–22, 2019): Novosibirsk, Publishing House of SB RAS, p. 207–210.
Viira, V., 2011, Lower and Middle Ordovician conodonts from the subsurface of SE Estonia and adjacent Russia: Estonian Journal of Earth Sciences, v. 60, p. 1–21.
Voldman, G.G., Albanesi, G.L., Alonso, J.L., Fernández, L.P., Banchig, A.L., Cardó, R., Ortega, G., and Vallaure, A.M., 2015, New conodont records from the Rinconada Formation, eastern margin of the Argentine Precordillera: tectono-stratigraphic implications: Stratigraphy, v. 12, p. 79–83.
Wang, Z.H., and Lou, K.Q., 1984, Late Cambrian and Ordovician conodonts from the marginal areas of the Ordos Platform, China: Bulletin of Nanjing Institute of Geology and Palaeontology, Academia Sinica, v. 8, p. 237–304. [In Chinese with English abstract]
Wang, Z.H., Qi, Y.P., and Wu, R.C., 2011, Cambrian and Ordovician Conodonts in China: Hefei, 388 p. [in Chinese with English summary]
Wang, Z.H., Bergström, S.M., Zhen, Y.Y., Zhang, Y.D., Wu, R.C., and Chen, Q., 2013, Ordovician conodonts from Dashimen, Wuhai in Inner Mongolia and the significance of the discovery of the *Histiodella* fauna: Acta Micropalaeontologica Sinica, v. 30, p. 323–343. [in Chinese with English abstract]

Zhen, Y.Y., 2020, Revision of the Darriwilian (Middle Ordovician) conodonts documented by Watson (1988) from subsurface Canning Basin, Western Australia: Alcheringa, v. 44, p. 217–252.
Zhen, Y.Y., 2021, Middle Ordovician conodont biostratigraphy of Australasia: Journal of Earth Science, v. 32, p. 474–485.
Zhen, Y.Y., and Percival, I.G., 2004, Middle Ordovician (Darriwilian) conodonts from allochthonous limestones in the Oakdale Formation of central New South Wales, Australia: Alcheringa, v. 28, p. 77–111.
Zhen, Y.Y., and Rutledge, J., 2020, Conodont biostratigraphy of the Ordovician turbiditic successions in New South Wales: Geological Survey of New South Wales, Report GS2020/0459, p. 1–57.
Zhen, Y.Y., Percival, I.G., and Webby, B.D., 2003, Early Ordovician conodonts from far western New South Wales, Australia. Records of the Australian Museum, v. 55, p. 169–220.
Zhen, Y.Y., Percival, I.G., Cooper, R.A., Simes, J.E., and Wright, A.J., 2009, Darriwilian (Middle Ordovician) conodonts from Thompson Creek, Nelson Province, New Zealand: Memoirs of the Association of Australasian Palaeontologists, v. 37, p. 25–53.
Zhen, Y.Y., Wang, Z.H., Zhang, Y.D., Bergström, S.M., Percival, I.G., and Chen, J.F., 2011, Middle to Late Ordovician (Darriwilian–Sandbian) conodonts from the Dawangou Section, Kalpin area of the Tarim Basin, northwestern China: Records of the Australian Museum, v. 63, p. 203–266.
Zhen, Y.Y., Normore, L.S., Dent, L.M., and Percival, I.G., 2020a, Middle Ordovician (Darriwilian) conodonts from the Goldwyer Formation of the Canning Basin, Western Australia: Alcheringa, v. 44, p. 25–55.
Zhen, Y.Y., Zhang, Y.D., Harper, D.A.T., Zhan, R.B., Fang, X., Wang, Z.H., Yu, S.Y., and Li, W.J., 2020b, Ordovician successions in southern-central Xizang (Tibet), China—refining the stratigraphy of the Himalayan and Lhasa terranes: Gondwana Research, v. 83, p. 372–389.
Zhen, Y.Y., Nicoll, R.S., Normore, L.S., Percival, I.G., Laurie, J.R., and Dent, L.M., 2021a, Ordovician conodont biostratigraphy of the Willara Formation in the Canning Basin, Western Australia: Palaeoworld, v. 30, p. 249–277.
Zhen, Y.Y., Percival, I.G., Gilmore, P., Rutledge, J., and Deyssing, L., 2021b, Conodont biostratigraphy of Ordovician deep-water turbiditic sequences in eastern Australia—a new biozonal scheme for the Open-Sea Realm: Journal of Earth Science, v. 32, p. 486–500.
Zhen, Y.Y., Laurie, J.R., Percival, I.G., Nicoll, R.S., and Cooper, B.J., in press, Ordovician conodonts from the Horn Valley Siltstone of the Amadeus Basin, central Australia: Australasian Palaeontological Memoirs, v. 56.

Accepted: 19 March 2022